Environmental Science & Technology

pubs.acs.org/est

Article

Humic and Fulvic Acid Fractions Differentially Regulate Methane-Dependent Arsenate Reduction in Paddy Soils

Yu Zhang, Yun Chen, Fengjie Liu, Yves Plancherel, Andreas Kappler, Lina Zou, Olubukola Oluranti Babalola, Ayansina Segun Ayangbenro, and Xianjin Tang*

Cite This: *Environ. Sci. Technol.* 2026, 60, 10804–10815

Read Online

ACCESS | Metrics & More | Article Recommendations | Supporting Information

ABSTRACT: Arsenic (As) contamination in paddy soils threatens global food security because microbial reduction of arsenate (As(V)) to mobile arsenite (As(III)) drives As mobilization. Methane (CH_4)-dependent As(V) reduction (M-AsR) is a key route coupling CH_4 cycling to As release, yet how structurally distinct soil organic matter (SOM) fractions regulate this pathway remains poorly understood. Here we show that an aromatic, quinone-rich humic acid fraction enhances electron transfer and promotes coupling of CH_4 oxidation to As(V) reduction, accelerating iron (Fe)-As mineral dissolution and increasing As(III) release by ∼1.5-fold. Accordingly, copy numbers of NC10-targeted *pmoA*, ANME-2d-targeted *mcrA*, and *arrA* increased by 116.6%, 126.5%, and ∼2.4-fold, respectively. In contrast, a carboxyl-rich fulvic fraction promoted acetate accumulation, thereby making CH_4-driven metabolism thermodynamically unfavorable. NC10-targeted *pmoA* and ANME-2d-targeted *mcrA* signals consequently decreased by 95.3% and 89.6%, respectively, and M-AsR was largely blocked, with the CH_4-driven As(III) component increasing by only 47.9%. Crucially, humic acid acts as an electron shuttle linking CH_4 oxidation and As(V) reduction, while fulvic acid disrupts this coupling process via acetate accumulation, highlighting the need for molecular-level SOM characterization to predict As risks in flooded soils.

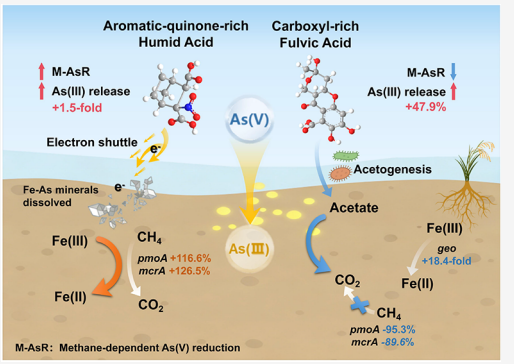

KEYWORDS: *arsenic, humic substances, methane, anoxic, paddy soil*

1. INTRODUCTION

Arsenic (As) contamination in flooded paddy soils is intensified by microbially mediated reduction of As(V) to the more mobile and toxic As(III), increasing dissolved As and threatening global food security.[1,2] Recent work has identified methane (CH_4)-dependent As(V) reduction (M-AsR) as a pathway in which CH_4 oxidation provides reducing equivalents to As(V)-reducing microorganisms, thereby amplifying CH_4-linked As(III) accumulation under anoxia.[3] This coupling is closely tied to dissolution of Fe−As minerals,[4] yet how soil organic matter modulates the magnitude and efficiency of M-AsR remains unclear. Defining this control is essential for predicting CH_4-amplified dissolved As(III) release and for informing mitigation strategies in paddy systems.

Humic substances are often reported to comprise a major fraction of soil organic matter and to participate in redox reactions through measurable electron-donating and electron-accepting capacities.[5−7] In practice, "humic acid", "fulvic acid", and "humin" are operational fractions defined by alkaline extraction and acid precipitation, and humic and fulvic fractions are commonly viewed as the more reactive extractable components under anoxia.[8] Humic acid is typically enriched in aromatic and quinone-like structures that support reversible redox cycling and electron shuttling.[9] Fulvic acid is generally lower in molecular weight and richer in carboxyl groups, enhancing solubility; however, its redox activity is often more variable and context-dependent than humic acid, depending on source material and functional-group distribution.[10] These contrasts suggest that the two fractions could impose distinct controls on M-AsR, yet mechanistic evidence within an integrated M-AsR system remains limited. Humic acid has been proposed to accept or relay electrons during anaerobic CH_4 oxidation (AOM), potentially linking CH_4 consumption to Fe(III) reduction and associated As mobilization.[11,12] Consistent with a microbial route for this effect, genome-resolved SIP in flooded paddy soil shows that soil humic acid can enrich potentially active dissimilatory As(V)-reducing bacteria (including *arrA*-harboring populations), underscoring that humic substances can shape As(V) respiration beyond purely sorptive effects.[13] Fulvic acid, by contrast, has been discussed mainly as a mobilizing ligand, enhancing reductive

Received: September 15, 2025
Revised: March 24, 2026
Accepted: March 25, 2026
Published: April 3, 2026

dissolution and desorption through complexation, acidity, and competition for mineral surface sites—mechanisms analogous to low-molecular-weight organic acids.[14,15] Most support for these roles comes from isolated redox or sorption reactions, leaving it unclear how each fraction reshapes the coupled CH_4–Fe-As network that underpins M-AsR. This gap matters because rice paddies are a major anthropogenic CH_4 source and are also prone to strong As mobilization under flooding.[16,17]

Microbial interactions among methanogens (CH_4 supply), CH_4 oxidizers (CH_4 consumption), Fe(III) reducers, and As(V) reducers underpin M-AsR in flooded soils and paddy systems.[18−20] Together, these guilds enable electron transfer from CH_4 oxidation to terminal electron acceptors such as As(V) and Fe(III). Accordingly, in this study, CH_4-linked genetic potential was tracked using NC10-targeted *pmoA* and ANME-2d-targeted *mcrA*,[21] respiratory As(V)-reduction potential was assessed using *arrA*, detoxification-associated As(V)-reduction potential was assessed using *arsC*, and Geobacteraceae abundance was tracked using a Geobacteraceae-targeted 16S rRNA gene assay relevant to Fe(III)-reducing consortia.[13] Metagenomic evidence further suggests that *Candidatus* Methanoperedens (ANME-2d) can dominate AOM and link CH_4 oxidation to Fe(III) reduction via reverse methanogenesis.[22] These archaea may employ multiheme c-type cytochromes to transfer electrons from CH_4 to extracellular Fe(III) (oxyhydr)oxide minerals, producing Fe(II) that triggers the reductive dissolution of As-bearing minerals.[4,23] Yet it remains unclear how humic acid versus fulvic acid reshapes these microbial interactions and, in turn, M-AsR-driven As mobilization.

Humic and fulvic amendments may also regulate M-AsR indirectly by promoting the accumulation of labile carbon intermediates, including acetate, which could compete with CH_4 and redirect electron flow.[24] A critical but underexplored aspect is the thermodynamic hierarchy that can shape electron-donor use during As(V) reduction. Under standard conditions, the CH_4-dependent pathway ($CH_4 + As(V) \rightarrow As(III) + CO_2$) yields a Gibbs free energy change (ΔG^0) of -276.7 kJ mol^{-1}, whereas acetate-driven reduction ($CH_3COO^- + As(V) \rightarrow As(III) + 2CO_2$) releases -580.6 kJ mol^{-1}, indicating a stronger energetic drive for acetate.[25] This contrast predicts that when acetate accumulates alongside CH_4, consortia may preferentially use acetate, potentially suppressing M-AsR—a hypothesis that has not been directly tested for acetate accumulation associated with humic- or fulvic-fraction amendment. To address this gap, we investigated how structurally distinct humic- and fulvic-acid fractions regulate M-AsR in flooded paddy soils, and we additionally conducted an independent acetate-amendment experiment to test whether acetate accumulation can weaken M-AsR. We aimed to (i) quantify how humic and fulvic fractions alter M-AsR and identify the dominant geochemical drivers, and (ii) resolve how key microbial guilds and functional genes track the observed shifts. Collectively, these experiments define how structurally distinct humic fractions regulate M-AsR through coupled geochemical and microbial controls, with implications for anticipating and mitigating As mobilization risk in flooded paddy soils.

2. MATERIALS AND METHODS

2.1. Experimental Preparation

Soil was collected from the plow layer (0−20 cm) of a paddy field in Shaoxing, Zhejiang Province, China (30°0′24.01″ N, 120°46′20.68″ E). After collection, plant debris and gravel were removed by sieving, and the soil was transported to the laboratory on ice. The homogenized soil was subsequently subdivided into two subsamples: one was air-dried for physicochemical characterization and incubation experiments, and the other was preserved at 4 °C to maintain microbial activity. Basic soil properties are summarized in Table S1. All chemicals were of analytical grade (or higher) unless otherwise stated. Commercial humic acid and fulvic acid (Shanghai Yuanye Bio-Technology Co., Ltd., China) were used as operational and chemically contrasting model amendments to represent humic-like redox-active versus fulvic-like carboxyl-rich and soluble traits within extractable soil organic matter. These organic fractions underwent rigorous spectroscopic characterization using Fourier transform infrared spectroscopy (FTIR; Thermo Fisher Scientific Nicolet iS20, USA) and solid-state ^{13}C nuclear magnetic resonance spectroscopy (^{13}C NMR; 400 MHz, Bruker Avance III HD, Germany). Spectra and corresponding functional-group assignments are shown in Figure S1. The electron-donating capacity and accepting capacity (EDC and EAC) were measured following the methods in SI.[26] Synthetic scorodite was prepared by controlled crystallization under acidic conditions following published methods.[27] All sterile water and mineral media were boiled and cooled under an argon atmosphere before use to minimize dissolved oxygen. Resazurin was included as a redox indicator, and no obvious color change was observed during incubation.

2.2. Laboratory Incubation

2.2.1. Experiment 1#. Effects of humic acid and fulvic acid on M-AsR in soil microcosms.

First, Supporting Experiment 1 verified that the M-AsR process in the tested soil followed the expected stoichiometry (SI). We then assessed the effects of humic acid and fulvic acid on M-AsR in anoxic soil suspensions. Specifically, two comparative groups were established by adding $^{13}CH_4$ (10%, v/v) or Ar to the headspace. Humic acid or fulvic acid (1% of soil dry weight) was supplemented to separate treatments, with sterile water as the control.[24,28] All systems contained 66.67 μM As(V) (5 mg L^{-1}) in 40 mL soil suspension medium (pH 6.2), consistent with the initial conditions of Supporting Experiment 1. Six treatments (five replicates each) were prepared identically under anoxic conditions using repeated vacuum−argon cycles. Incubations were conducted in the dark at 25 °C with shaking at 150 rpm. Temporal changes in aqueous As species and headspace $^{13}CH_4$/$^{13}CO_2$ were monitored on days 0, 1, 3, 6, and 9.

2.2.2. Experiment 2#. Mechanistic differentiation of humic- and fulvic-fraction effects on M-AsR.

To resolve how humic acid and fulvic acid differentially regulate M-AsR under simulated paddy-soil conditions, we established six microcosm treatments and monitored them for 21 days: sterile water + $^{13}CH_4$, sterile water + Ar, humic acid + $^{13}CH_4$, humic acid + Ar, fulvic acid + $^{13}CH_4$, fulvic acid + Ar. Microcosms were prepared in 60 mL serum bottles with 10.0 g (dry weight) soil and 20 mL anoxic solution containing humic acid or fulvic acid at 1% (w/w, dry soil basis), or sterile water as a control. After 30 min argon sparging, bottles were sealed with butyl rubber stoppers, with three treatments receiving 4 mL $^{13}CH_4$ (gas displacement) to evaluate M-AsR activity, while Ar controls assessed CH_4-independent As(V) reduction. Each treatment was run with six replicates and incubated statically at 25 °C in the dark. Headspace gas concentrations were monitored at 0, 3, 7, 14, and 21 days before destructive sampling. Soils were split for DNA analysis (−80 °C) and porewater extraction by centrifugation (3100*g*, 10 min). Supernatants were filtered (0.22 μm), acidified with 6 M HCl (1% v/v) to stabilize As and Fe species, and stored at −20 °C until analysis.[29] To probe Fe-mineral involvement in humic-acid−mediated M-AsR, we performed validation experiments using synthetic scorodite (protocols in the SI) as a chemically defined

https://doi.org/10.1021/acs.est.5c12983
Environ. Sci. Technol. 2026, 60, 10804−10815

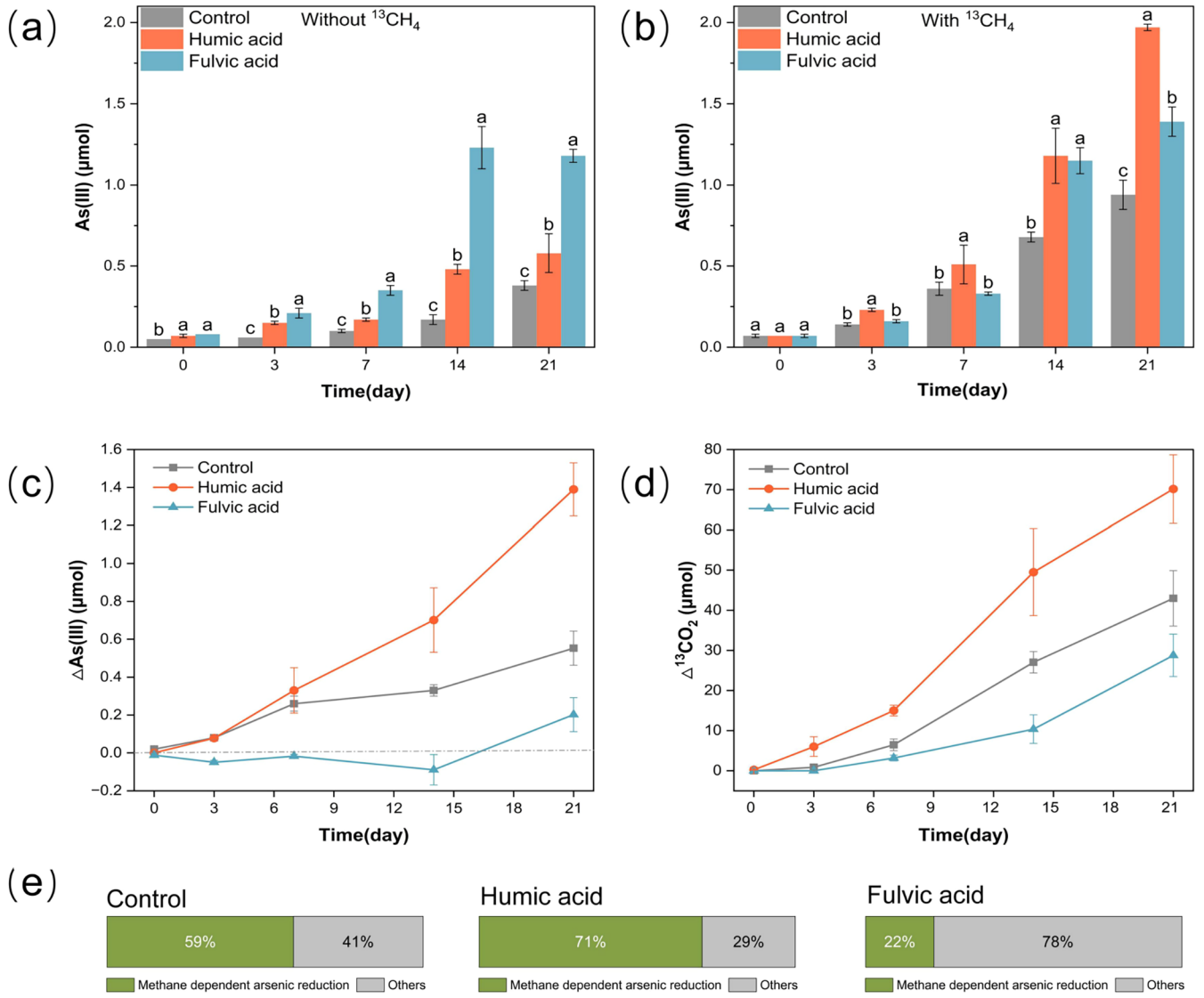

Figure 1. Humic acid strengthens, whereas fulvic acid weakens, CH_4-dependent As(V) reduction pathway (M-AsR) in paddy-soil microcosms. Time courses of dissolved As(III) under $^{13}CH_4$ or Ar headspace in microcosms amended with humic acid or fulvic acid (a, b). Molar concentration differences of As(III) (c) and cumulative $^{13}CO_2$ (d) (sum of liquid and gaseous phases) under treatments with or without $^{13}CH_4$. Contribution rates (%) of the M-AsR to As(III) accumulation was calculated as ((treatment-$^{13}CH_4$) - (treatment-Ar))/(treatment-$^{13}CH_4$) × 100 (e). For example, for humic acid, ((Humic acid-$^{13}CH_4$) - (Humic acid-Ar))/(Humic acid-$^{13}CH_4$) × 100. Error bars represent standard deviations (n = 6). Different letters represent statistically significant differences (p < 0.001).

Fe−As phase to isolate Fe-coupled dissolution and associated As release.

2.2.3. Experiment 3#. Effects of acetate concentration on M-AsR.

We performed an acetate-gradient microcosm experiment to isolate acetate effects on M-AsR and quantify competition with CH_4 independent of humic- or fulvic-acid additions. Acetate solutions at 0, 1, 3, and 6 mM (Hangzhou Bangyi Chemical Co., Ltd., China) were used to establish eight treatment groups: sterile-water controls amended with either $^{13}CH_4$ or Ar, and acetate treatments (1/2/6 mM) likewise amended with either $^{13}CH_4$ or Ar. Each treatment was conducted with six replicates. For each microcosm, 10.0 g (dry weight) soil was thoroughly mixed with the designated acetate solution or sterile water in a 60 mL serum bottle. After deoxygenation by argon purging, 4 mL of $^{13}CH_4$ was injected to achieve a 10% (v/v) headspace concentration, followed by static incubation at 25 °C for 21 days. Headspace gases and porewater As(III) were measured on days 0, 3, 7, 14, and 21.

2.3. Chemical Analysis

Headspace $^{13}CH_4$ and $^{13}CO_2$ were measured on an Agilent 6890N/5975B GC-MS equipped with an HP-PLOT U column (30 m × 0.32 mm × 10 μm). Samples were injected at 10 μL, and spiked standards were run every 20 samples for quality control; dissolved-gas concentrations were calculated using Henry's law. As species (As(III), As(V), DMA, and MMA) were quantified by HPLC-ICP-MS (Agilent 1260 HPLC coupled to a PerkinElmer NexION 300X) using a PRP X-100 column (250 mm × 4.1 mm) and 20 mM $NH_4H_2PO_4$ (pH 6.5) as the mobile phase. Calibration was verified with 50 μg L^{-1} standards every 10 samples (detection limit: 0.490 μg L^{-1}). Total As/Fe/Mn concentrations were determined by ICP-MS after microwave digestion (HNO_3−HF-H_2O_2, 4:2:2 v/v) of 0.2 g soil, achieving >95% recovery using GBW07405 certified soil. Soil pH and redox potential (Eh) were measured with a Mettler Toledo FE28 probe, while dissolved organic carbon (DOC) and total nitrogen (TN) were analyzed by Multi N/C 3100 TOC/TN analyzer. Fe(II) was assessed via 1,10-phenanthroline spectrophotometry at 510 nm, and acetate

https://doi.org/10.1021/acs.est.5c12983
Environ. Sci. Technol. 2026, 60, 10804−10815

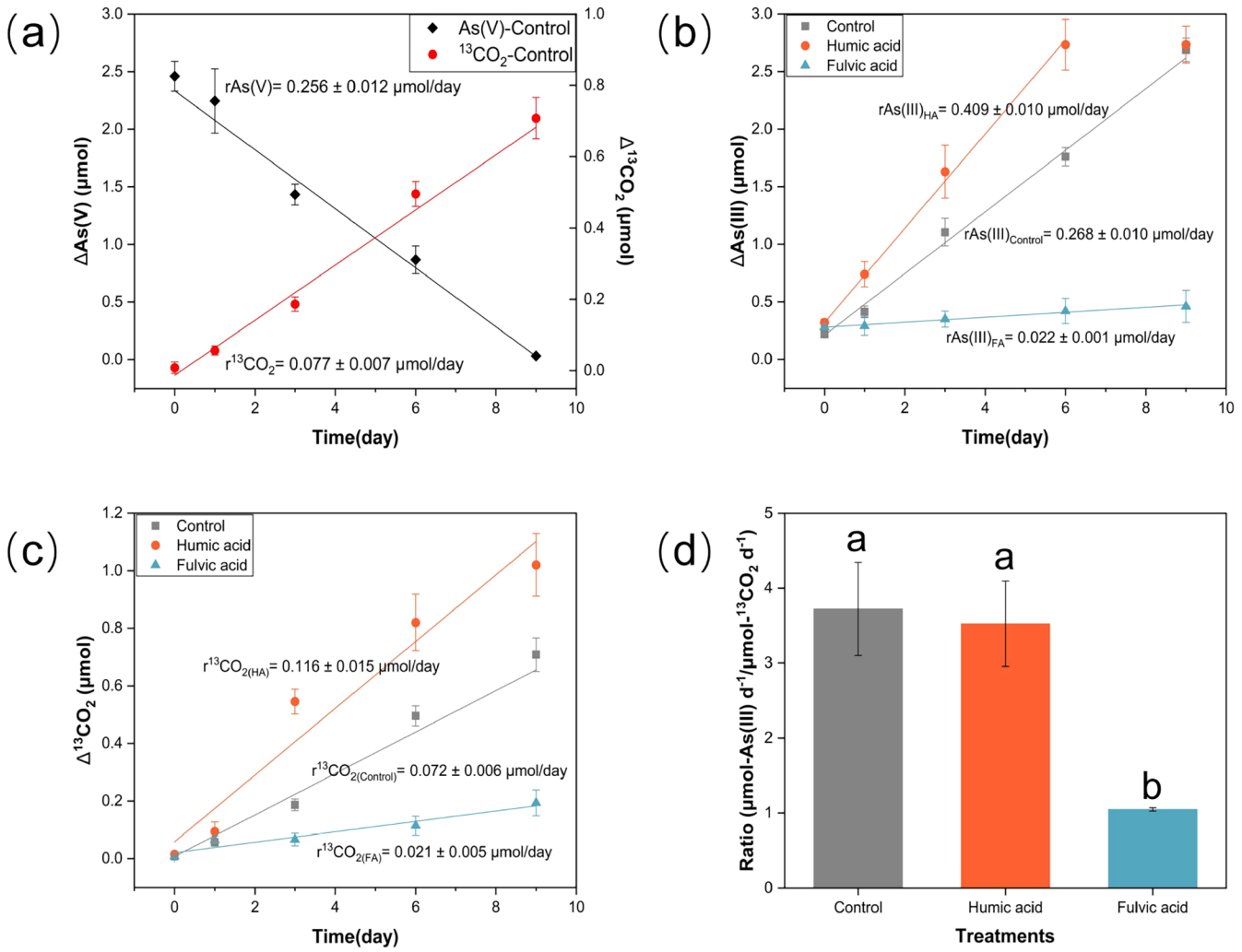

Figure 2. Humic acid and fulvic acid differentially regulate the kinetics and stoichiometry of CH_4-dependent As(V) reduction (M-AsR). Electron balance between $^{13}CH_4$ oxidation and CH_4-oxidation-driven As(V) reduction (a); Net As(III) accumulation (b) and $^{13}CO_2$ production (c) in quinone-rich humic acid, carboxyl-rich fulvic acid, and control treatments; M-AsR rate ratios (d). Net $^{13}CO_2$ production calculated as the difference between As(V)-amended and As(V)-free (Ar) systems. Net As(III) concentrations represent differences between $^{13}CH_4$-supplemented and $^{13}CH_4$-free (Ar) conditions. Error bars were standard deviations (n = 5).

concentrations were determined using Agilent 1260 HPLC with Hi-Plex H column.

2.4. Microbial Analysis

Soil DNA was extracted with the TIANGEN Soil Genomic DNA Extraction Kit (DP336; TIANGEN Biotech Co., Ltd., Beijing, China) according to the manufacturer's instructions. DNA quality was verified through 2% agarose gel electrophoresis, and qualified extracts were stored at −80 °C prior to downstream analyses. The hypervariable V4 region of the 16S rRNA gene was amplified in triplicate using primers 515F (GTGCCAGCMGCCGCGGTAA) and 806R (GGACTACHVGGGTWTCTAAT),[30] with thermal cycling conditions adapted from established methods to minimize amplification bias.[31] Triplicate amplicons from each soil were pooled, and DNA concentrations were quantified using a Qubit 3.0 Fluorometer (Thermo Fisher Scientific, USA) with the dsDNA HS Assay Kit. Amplicon libraries were subsequently constructed and sequenced on an Illumina NovaSeq 6000 platform (Illumina, San Diego, USA) for high-throughput parallel sequencing with a paired-end 250 bp (PE250) mode by Kaitai Biotechnology Co., Ltd. (Hangzhou, China). Raw sequences were processed using the DADA2 pipeline (v1.22) in R to generate amplicon sequence variants (ASVs).[32] Taxonomic assignment was performed against the SILVA 138.1 database with an 80% confidence threshold. ASV tables were rarefied to 30,000 reads per sample for downstream analyses. Representative ASVs underlying key methanotroph-affiliated assignments were further checked by BLAST for conservative interpretation of genus-level taxonomy. The 16S rRNA gene sequences reported in this paper have been deposited in NCBI SRA under accession No. PRJNA1418327. Real-time quantitative PCR (qPCR) was conducted to quantify primer-defined targets associated with As, CH_4, and Fe cycling as proxies for genetic potential. For CH_4-linked pathways, we quantified an NC10-targeted *pmoA* assay and an ANME-2d-targeted *mcrA* assay. We also quantified *arrA*, *arsC*, and a Geobacteraceae-targeted 16S rRNA gene assay to assess respiratory As(V)-reduction potential, detoxification-associated cytosolic As(V)-reduction potential, and Geobacteraceae abundance relevant to Fe(III)-reducing consortia, respectively. These assays were interpreted according to primer scope rather than as universal proxies for the corresponding processes or lineages. Primer sequences and original references are summarized in Table S2.[21,33]

2.5. Statistical Analysis

Figures were prepared in Origin 2024b. Random forest regression was performed in R using rfPermute (v2.5.1) to identify predictors of aqueous As(III) dynamics; variable importance was evaluated as the percentage increase in mean squared error (%Inc.MSE).[34] Redundancy analysis (RDA) was conducted in R using the microeco

https://doi.org/10.1021/acs.est.5c12983
Environ. Sci. Technol. 2026, 60, 10804−10815

package, where key environmental factors were selected through forward selection (VIF < 10) and modeled via trans_rda() after Hellinger transformation of microbial data. The triplot visualization integrating samples, species, and environmental vectors was generated with ggplot2, with axis variance explained annotated and statistical significance ($p < 0.01$) verified by 999 permutations. Differences among treatments were evaluated by one-way ANOVA with Tukey's HSD posthoc test ($p < 0.05$) using SPSS 27 (IBM Corp., Armonk, NY, USA).

3. RESULTS AND DISCUSSION

3.1. Humic Acid, but Not Fulvic Acid, Enhanced M-AsR

Both humic acid and fulvic acid amendments increased dissolved As(III) relative to the unamended control (Figure 1a). Isotope tracing with $^{13}CH_4$, however, revealed contrasting coupling to CH_4 oxidation between the two soil organic matter fractions. With humic acid, $^{13}CH_4$ increased As(III) by ∼1.5-fold and elevated $^{13}CO_2$ production by 63.2% relative to the Ar control (Figure 1c,1d), raising the inferred CH_4-driven contribution to As(III) formation from 59% to 71% (Figure 1e). In contrast, fulvic acid produced indistinguishable As(III) concentrations under $^{13}CH_4$ and Ar ($p > 0.05$; Figure 1a,1b) and reduced the inferred CH_4-driven contribution to 22% (Figure 1e). Consistent with this weak isotope separation, the CH_4-driven As(III) component increased by only 47.9% under fulvic acid.

Together, these isotope-resolved responses indicate that humic acid selectively strengthens M-AsR, whereas fulvic acid largely decouples As(III) accumulation from CH_4 oxidation or diverts electron flow away from the CH_4-driven pathway. We therefore treat the contrasting outcomes as a chemistry-defined switch in pathway coupling: humic acid is consistent with redox-active functionalities that can support extracellular electron transfer and sustain CH_4-derived electron throughput to As(V) reducers,[35,36] whereas fulvic acid is consistent with a less redox-active, more carboxyl-enriched fraction that shifts electron allocation toward competing sinks.[37,38] The mechanistic basis for this divergence is tested in the following sections using molecular characterization, electron-transfer metrics, Fe mobilization, and microbial functional responses.

3.2. Quinone Moieties Accelerated While Carboxyl Groups Disrupted M-AsR Efficiency

In the unamended control (no added organic matter fraction), As(V) reduction and CH_4 oxidation proceeded in a coupled manner (Figure 2a). As(V) reduction proceeded at 0.256 ± 0.012 μmol day^{-1} alongside $^{13}CO_2$ production at 0.077 ± 0.007 μmol day^{-1}, yielding a $\Delta[As(III)]/\Delta[^{13}CO_2]$ ratio of 3.32:1—close to the theoretical 4:1 stoichiometry expected for CH_4 oxidation coupled to As(V) reduction in wetland sediments.[3] Sustained CH_4 consumption (0.082 ± 0.004 μmol day^{-1}; data not shown) supports CH_4 as the dominant electron donor, whereas the modest deviation from theory is consistent with residual competing electron acceptors (e.g., Fe(III)) intercepting part of the electron flux.[22,39]

Humic acid increased the throughput of this coupled metabolism without changing its stoichiometric signature (Figure 2b–d). As(III) production accelerated to 0.409 ± 0.010 μmol day^{-1} (+52.6% versus control), and As(V) was nearly exhausted by Day 6 (<0.05 μmol residual). In parallel, $^{13}CO_2$ production increased to 0.116 ± 0.015 μmol day^{-1} (+61.1% versus control), while the $\Delta[As(III)]/\Delta[^{13}CO_2]$ ratio remained near the expected range (3.85 ± 0.21; $p > 0.05$ versus theory), indicating an acceleration of M-AsR rather than a rerouting of the reaction network (Figure 2d). Consistent with this interpretation, humic acid exhibited quinone-associated features in FTIR and solid-state ^{13}C NMR (1608 cm^{-1}; aromatic carbon at 110–160 ppm; quinone carbonyl at ∼180 ppm; Figure S1) and substantial carbon-normalized EDC and EAC (Figure S6), supporting that the material is redox-active and capable of mediating electron exchange in these microcosms. Quinone-enriched structures have been proposed to accelerate interspecies electron transfer between CH_4 oxidizers and metal-reducing microorganisms.[40,41] Notably, these bulk assays do not resolve the specific redox moieties operating in situ or quantify electron-shuttling fluxes directly; thus, electron shuttling is treated here as a constrained, testable explanation rather than a definitive assignment. Beyond redox shuttling, humic acid could enhance the apparent M-AsR signal through indirect pathways. On the biological side, humic amendments may increase the size and activity of the relevant functional guilds by providing slowly utilizable organic substrates and/or by complexing micronutrients, thereby elevating community-level metabolic capacity and raising baseline rates of CH_4 turnover and coupled metal(loid) reduction.[42] On the geochemical side, humic substances can reshape Fe–As interfacial chemistry via adsorption/coating and aggregation effects that alter surface charge and reactive-site availability, promote competitive desorption of As(V), and increase the accessibility and reducibility of Fe(III)-bearing phases, collectively facilitating Fe–As phase transformation and As(III) release.[43,44]

Fulvic acid, in contrast, strongly suppressed the coupled process (Figure 2b–d). As(III) production decreased to 0.022 ± 0.001 μmol day^{-1} (8.2% of control), and $^{13}CO_2$ production fell to 0.021 ± 0.005 μmol day^{-1} (29.2% of control). Critically, this suppression coincided with substantial acetate accumulation (97.22 ± 13.34 mg L^{-1}, Figures 2d and S2) and a pronounced distortion of the $\Delta[As(III)]/\Delta[^{13}CO_2]$ ratio ($p < 0.01$), consistent with decoupling of CH_4 oxidation from As(V) reduction. Given acetate's thermodynamic and kinetic advantages as an electron donor in aqueous systems, acetate accumulation is expected to competitively draw As(V)-reducing capacity away from CH_4-linked electron flow, thereby lowering M-AsR efficiency under fulvic acid amendment.[33]

3.3. Humic Acid Promoted Fe–As Mineral Dissolution under CH_4-Amended Conditions

Multivariate analyses were used to identify which measured geochemical variables covaried most strongly with dissolved As(III) across treatments (Figure S3). Random forest ranked total dissolved As, porewater ferrous iron (Fe(II)), and acetate as the strongest statistical predictors of As(III) variability (18.5%, 16.3%, and 15.7% of explained variance, respectively; Figure S3b), and Pearson correlations independently confirmed positive associations among these variables ($p < 0.001$; Figure S3a). Notably, acetate emerged as one of the strongest predictors of aqueous As(III), consistent with the pronounced acetate accumulation observed in fulvic-acid-amended incubations (see Figure 5a,5b below). Because these approaches quantify association rather than causality, we use them here to prioritize interpretation of directly measured Fe and As dynamics. Across all incubations, As(III) dominated the dissolved As pool (>97%; Figure S4), and its temporal pattern closely tracked total dissolved As, consistent with reductive mobilization controlling dissolved As accumulation under anoxia.

https://doi.org/10.1021/acs.est.5c12983
Environ. Sci. Technol. 2026, 60, 10804–10815

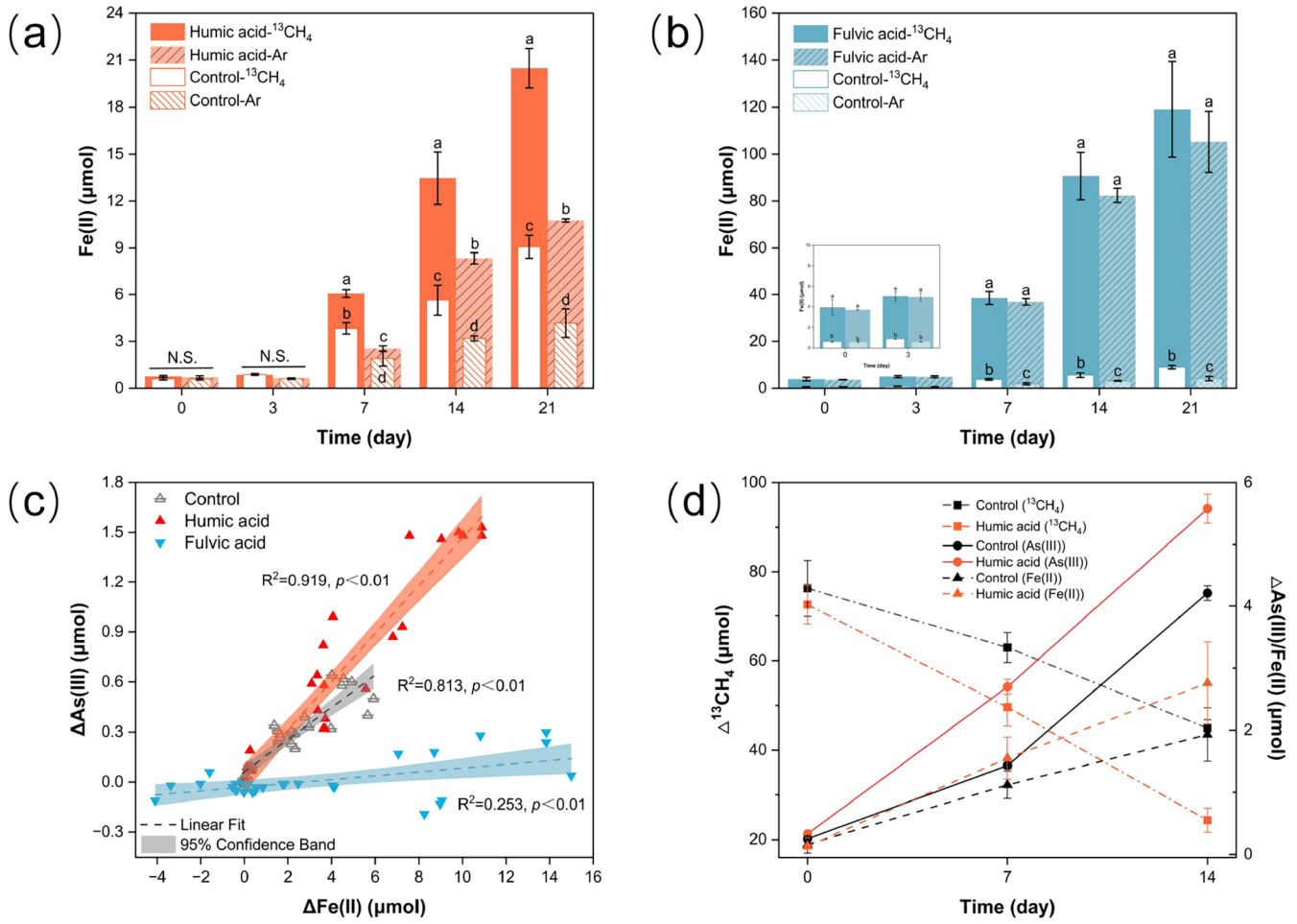

Figure 3. Dynamics of iron (Fe) in soil porewater under different treatments. Effects of humic acid and fulvic acid on Fe(II) content (a, b). Linear regression between ΔAs(III) and ΔFe(II) (95% confidence interval) (c). Changes in the release of As(III) and Fe(II) from scorodite driven by CH_4 oxidation by humic acid and the decrease in $^{13}CH_4$ concentration (d). Error bars represent standard deviations (n = 6). Different lowercase letters denote significant differences (p < 0.05).

We therefore tested whether treatment-dependent Fe reduction tracked differences in dissolved As mobilization (Figure 3a–c). Porewater Fe(II), used here as an indicator of net Fe(III) reduction, was 125.6% higher in humic-acid microcosms than in the unamended control (Figure 3a). Within the humic-acid treatment, CH_4 addition further increased Fe(II) by 47.4% relative to the Ar control (Figure 3a), indicating that the CH_4-amended condition coincided with stronger Fe reduction. In contrast, fulvic acid showed no consistent CH_4-dependent separation in Fe(II) over time (p > 0.05), with a divergence observed only at Day 21 (Figure 3b). The empirical coupling between Fe reduction and dissolved As release also differed among treatments: the slope of ΔAs(III) versus ΔFe(II) increased under humic acid (0.144) relative to the control (0.096), whereas fulvic acid markedly weakened this coupling (0.011; Figure 3c). Together, these measurements support that humic acid strengthens Fe reduction and tightens Fe–As comobilization, particularly under CH_4-amended conditions. This pattern is consistent with prior reports that quinone-rich humic materials can facilitate microbial dissimilatory Fe reduction and that CH_4-oxidation partners (or CH_4-derived metabolites) can enhance Fe-reducing activity within anoxic consortia;[7,22,45] however, we directly quantify Fe(II) and dissolved As responses here, not the underlying electron-transfer routes.

To more directly test whether Fe–As mineral dissolution can account for humic-acid–associated As release, we conducted parallel incubations using synthetic scorodite as a chemically defined Fe–As endmember (Figure 3d). Humic acid increased CH_4 oxidation activity by 54.1% and this increase co-occurred with higher dissolved As(III) (+32.5%) and Fe(II) (+43.0%) (Figure 3d), consistent with enhanced reductive dissolution of the Fe–As phase under conditions that promote Fe reduction. In this framework, Fe(II) accumulation is interpreted as reflecting increased Fe(III) reduction, and the coordinated rise in dissolved Fe(II) and As(III) is interpreted as evidence for Fe-coupled As release;[46] we do not directly measure mineral dissolution rates in soil, and thus "dissolution" is inferred from dissolved release patterns and the endmember behavior. Scorodite represents a simplified single-phase system and does not capture heterogeneous Fe mineral assemblages, reactive coatings, and microscale sorption environments in paddy soils; accordingly, these incubations are used to support mechanistic consistency rather than to extrapolate quantitative dissolution kinetics to field conditions.[47]

3.4. Dynamics of Soil Microbial Communities and Analysis of Functional Genes

Amplicon sequencing revealed that humic acid and fulvic acid reshaped the CH_4–As-Fe microbial consortium in opposite

https://doi.org/10.1021/acs.est.5c12983
Environ. Sci. Technol. 2026, 60, 10804–10815

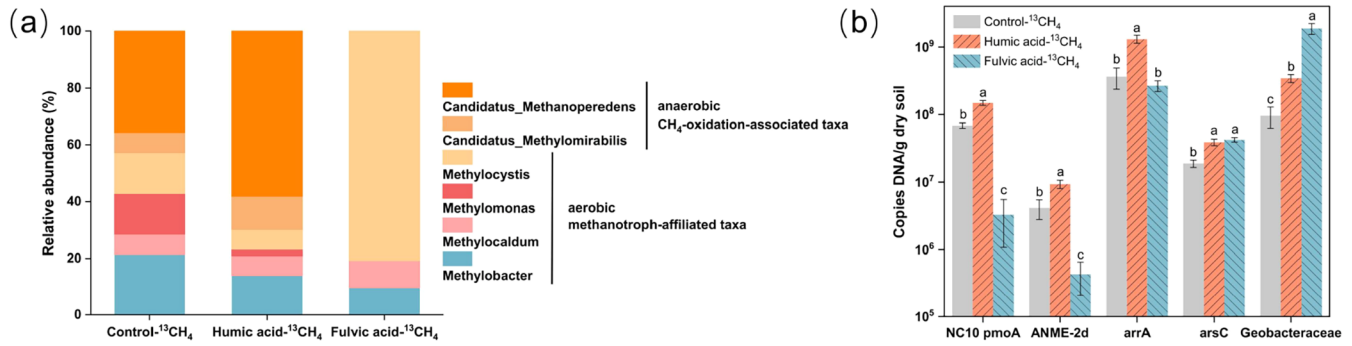

Figure 4. Humic and fulvic acids differentially remodel microbial consortia controlling the M-AsR process. Influence of humic acid and fulvic acid on the relative composition of selected CH_4-turnover-associated taxa, normalized to 100% within the selected assemblage and assigned using BLAST-refined 16S rRNA gene taxonomy (a) and on targeted qPCR assays related to CH_4-linked pathways, As transformation, and Geobacteraceae abundance (b). Error bars represent standard deviations (n = 6). Different lowercase letters denote significant differences (p < 0.05).

directions (Figure 4a). Under humic acid amendment, aerobic methanotroph-affiliated taxa increased to ∼1.6-fold of the control, whereas anaerobic CH_4-oxidation-associated taxa increased to ∼ 6.0-fold of the control. Within these groups, sequences assigned to *Methylobacter*, *Candidatus methylomirabilis*, and *Candidatus methanoperedens* increased to ∼2.0-fold, ∼3.8-fold, and ∼6.7-fold of the control, respectively. Phylogenetic analysis showed 97.6% sequence similarity between the enriched ANME-2d sequences and *C. methanoperedens*, consistent with the presence of taxa capable of anaerobic CH_4 turnover in flooded soils.[48,49] In contrast, fulvic acid produced a divergent community response: sequences assigned to *Methylobacter* decreased by 73.3%, while NC10 bacteria and ANME-2d archaea fell below the detection limit, and *Bacillus* increased by 382.0% (Figures 4a and S5).

These shifts provide biological context for the isotope-resolved geochemical signals reported above, while we emphasize that amplicon data report relative abundance rather than in situ activity. The enrichment of aerobic methanotroph-affiliated taxa under humic acid is ecologically plausible even under anoxic incubation because flooded soils commonly sustain sharp microscale redox gradients. Although dissolved or headspace O_2 concentrations were not measured directly, destructive sampling showed that ORP remained low throughout incubation (−180 to −230 mV), indicating persistently reducing bulk conditions. However, trace O_2 (residual or minor ingress during handling) cannot be ruled out and, together with microscale redox gradients, may be sufficient to sustain aerobic methanotroph-affiliated taxa growth under oxygen-limited conditions.[50−52] Meanwhile, key anaerobic populations involved in CH_4−As/Fe coupling often grow slowly and may not become numerically dominant over the incubation time scale despite contributing substantially to electron flow and solute production. The simultaneous enrichment of NC10 offers an additional, testable explanation for CH_4 activation under oxygen limitation, because NC10 bacteria mediate nitrite-dependent AOM via an intra-aerobic pathway that generates intracellular O_2 equivalents for CH_4 oxidation chemistry.[53] The rise of ANME-2d-related archaea further supports the presence of anaerobic CH_4-turnover potential in flooded soils, consistent with enrichments from paddy field soils and known coupling of AOM to nitrate reduction in this lineage.[54] Therefore, the humic-acid enrichment of *Methylobacter*, NC10, and ANME-2d is consistent with a consortium that sustains CH_4-linked redox cycling and strengthens coupling among CH_4 turnover, Fe reduction, and As transformation. Conversely, the fulvic-acid enrichment of *Bacillus*, together with the decline in CH_4-oxidizer signals, is consistent with a shift toward fermentative carbon processing in which acetate is a common end product,[55] thereby reducing reliance on CH_4 as an electron donor and weakening the M-AsR. We tested this hypothesis directly in Section 3.5 using acetate dynamics and substitution tests.

As a complementary molecular line of evidence, qPCR showed that humic acid and fulvic acid shifted the targeted CH_4-linked assays in opposite directions (Figure 4b). Under humic acid, copy numbers of the NC10-targeted *pmoA* and the ANME-2d-targeted *mcrA* increased by 116.6% and 126.5%, respectively, consistent with enrichment of the targeted CH_4-linked pathways rather than with total methanotrophic or AOM potential. In the same treatment, *arrA* increased by 236.4%, whereas *arsC* increased by 106.4%, indicating enhanced respiratory and detoxification-associated As(V)-reduction potential, respectively.[56,57] The Geobacteraceae-targeted signal also increased by 257.3%, consistent with enrichment of a lineage commonly associated with extracellular electron transfer and Fe(III) reduction under anoxic conditions. In contrast, under fulvic acid, NC10-targeted *pmoA* and ANME-2d-targeted *mcrA* signals decreased by 95.3% and 89.6%, respectively, whereas *arsC* increased by 124.5% and the Geobacteraceae-targeted signal rose by ∼18.4-fold, with no increase in *arrA* (Figure 4b). Together, these patterns indicate that fulvic acid favored weaker selection for the targeted CH_4-linked and *arrA*-type respiratory pathways, while maintaining detoxification-associated As(V) reduction and enriching Geobacteraceae-related populations.[58] We emphasize that DNA-level copy numbers primarily reflect genomic capacity and are not expected to map directly onto transcriptional activity or in situ process rates, which in this study are constrained chiefly by isotope-based and porewater geochemical signals.

3.5. Acetate Accumulation Driven by Fulvic Acid Inhibits M-AsR via Substrate Competition

We tracked acetate dynamics to determine whether acetate accumulation in fulvic-acid-amended microcosms could reroute electron flow during incubations. In humic-acid-amended microcosms, acetate trajectories were comparable between the $^{13}CH_4$ and Ar conditions at each sampling time, indicating that humic acid did not impose a CH_4-dependent

https://doi.org/10.1021/acs.est.5c12983
Environ. Sci. Technol. 2026, 60, 10804−10815

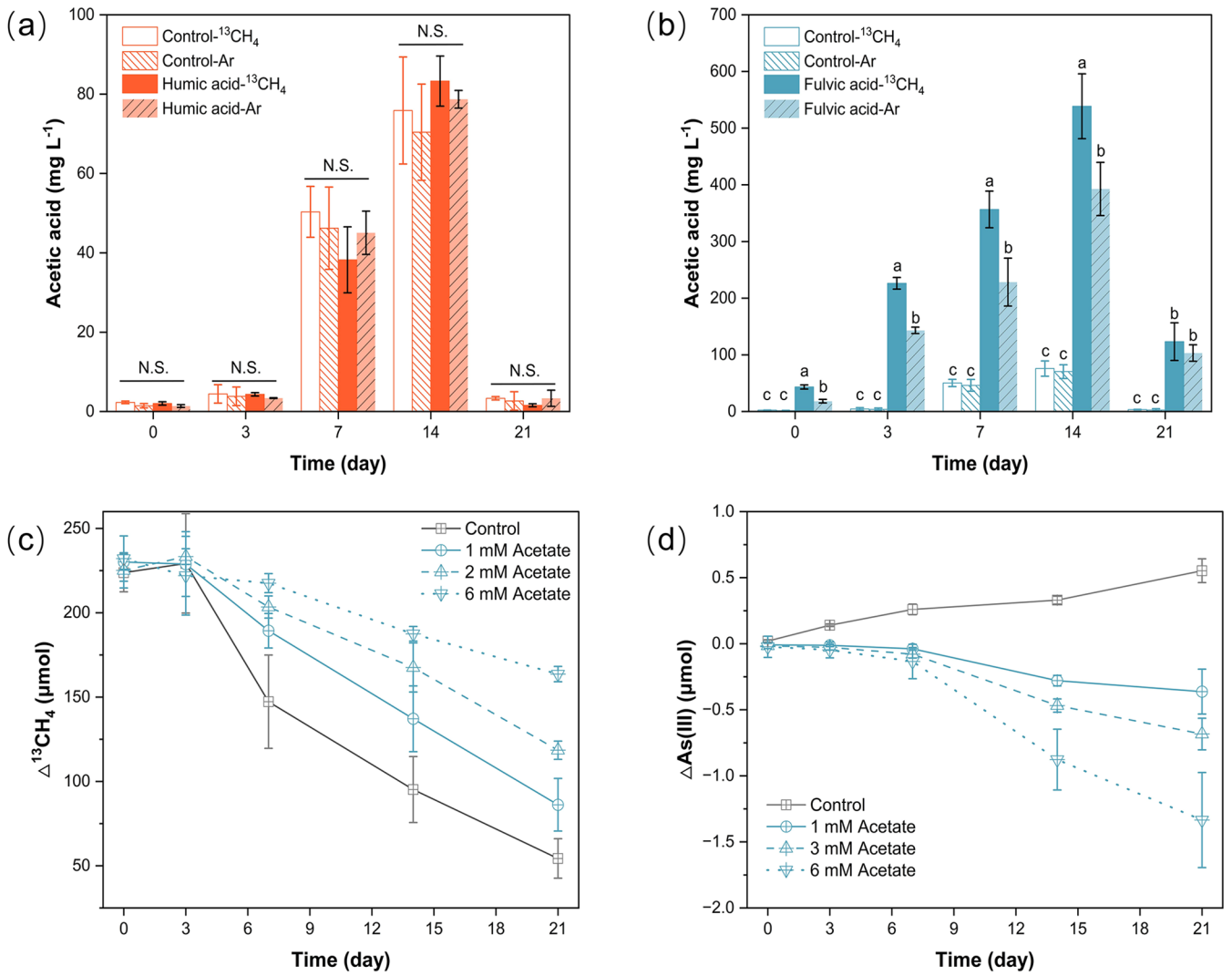

Figure 5. Acetate accumulation and acetate-amendment test reveal acetate-driven suppression of CH_4-dependent As(V) reduction (M-AsR). Acetate concentrations in microcosms amended with humic acid or fulvic acid and in unamended controls under $^{13}CH_4$ and Ar headspace (a, b). Headspace $^{13}CH_4$ in acetate-amended microcosms with 0, 1, 3, and 6 mM acetate (c). Net CH_4-linked As(III) accumulation expressed as ΔAs(III) in the acetate-amendment experiment (d). ΔAs(III) was calculated as the difference between the $^{13}CH_4$ and Ar incubations. Error bars represent standard deviations (n = 6). Different lowercase letters denote significant differences ($p < 0.05$).

shift in acetate availability (Figure 5a). In contrast, fulvic acid drove pronounced acetate accumulation (Figure 5b). Under $^{13}CH_4$, acetate was 37.2% higher than the corresponding Ar controls, and fulvic acid generated acetate concentrations up to 6.1-fold above the blank control even without CH_4 addition. Such acetate accumulation is consistent with prior observations that, under flooded or anoxic conditions, fulvic substances can promote microbial carbon processing and the formation of low-molecular-weight organic acids, notably acetate, whereas humic acids generally provide far less fermentable carbon and instead influence redox processes through redox-active moieties that facilitate extracellular electron transfer.[24] However, our data do not independently distinguish direct amendment-derived acetate from biologically generated acetate stimulated by the fulvic-acid amendment.

To test whether acetate itself can suppress the CH_4-linked component of As(V) reduction, we performed an acetate-amendment experiment spanning 0, 1, 3, and 6 mM. Increasing acetate slowed headspace $^{13}CH_4$ drawdown, corresponding to a 15.1−59.6% reduction in apparent $^{13}CH_4$ consumption relative to the acetate-free control (Figure 5c). In parallel, net As(III) accumulation attributable to CH_4, expressed as ΔAs(III), declined by 1.66−3.41-fold across the acetate gradient (Figure 5d). Together, the acetate time series and the substitution test show that an acetate pulse is sufficient to dampen CH_4 turnover and weaken the CH_4-linked contribution to As(V) reduction under our incubation conditions.

These results show that acetate accumulation is sufficient to suppress M-AsR in our microcosms. This suppression likely reflects substrate competition and kinetic/ecological advantages of acetate utilization, rather than thermodynamic favorability alone. Acetate is a preferred and rapidly utilized electron donor for diverse anaerobic respirers, including As(V)- and Fe-reducing populations,[59,60] and thus can redirect respiratory activity away from CH_4 oxidation even when CH_4 is available. Beyond this competition for electron flow, acetate can directly dampen CH_4 oxidation through regulatory constraints. In a peat-soil microcosm supplemented with the facultative methanotroph *Methylocella silvestris*, acetate repressed transcription of CH_4 monooxygenase and reduced

https://doi.org/10.1021/acs.est.5c12983
Environ. Sci. Technol. 2026, 60, 10804−10815

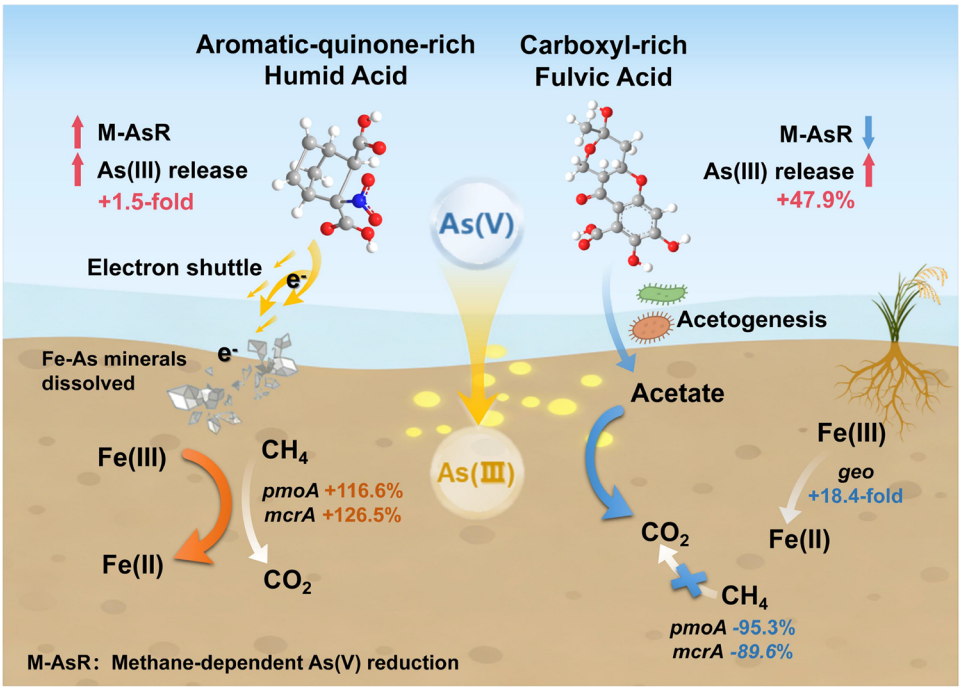

Figure 6. Proposed framework for how humic acid and fulvic acid differentially regulate CH_4-dependent As(V) reduction (M-AsR) and As mobilization in flooded paddy soil.

CH_4 oxidation, and DNA-SIP confirmed that this repression can operate in soils rather than only in pure culture.[61] Acetate additionally serves as a central precursor for CH_4 production in flooded soils; elevated acetate can stimulate acetoclastic methanogenesis and reorganize CH_4 cycling,[62] which can reduce the selective pressure for CH_4 oxidation and further loosen the coupling between CH_4 turnover and As(V) reduction. In this framing, acetate acts both as an alternative electron-donor currency for anaerobic respiration and as a driver of CH_4-production pathways that can compete ecologically with CH_4-oxidizing guilds.[33]

Importantly, acetate accumulation should not be treated as the only fulvic-acid control on M-AsR. Carboxyl-rich fulvic acid can modify mineral-solution partitioning of As by competing with As(V) for sorption sites on Fe (hydr)oxides, forming Fe-bridged organic complexes that stabilize dissolved Fe−As species, and altering interfacial charge and microscale redox niches that govern access to reactive Fe phases; in some settings, fulvic-derived redox-active groups may also contribute to M-AsR.[44,63] Thus, we treat acetate-driven substrate competition as a proximal constraint supported by the acetate-gradient tests, while recognizing that sorption/complexation and microenvironmental effects can act in parallel and may amplify decoupling of CH_4 oxidation from As(V) reduction. Likewise, thermodynamic favorability provides a feasibility boundary, but pathway selection in soils is shaped by kinetic and ecological constraints, including uptake and enzyme regulation, electron-acceptor accessibility at mineral surfaces, and community interactions.[64] We therefore use thermodynamics as a boundary condition to interpret directionality, not as a deterministic predictor of pathway dominance.

In conclusion, our laboratory incubations show that humic and fulvic acids can differentially regulate M-AsR in flooded paddy soil (Figure 6). Quinone-rich humic acid likely enhances electron shuttling and strengthens coupling between CH_4 oxidation and As(V) reduction, thereby stimulating M-AsR and associated As mobilization. By contrast, the more labile, carboxyl-rich fulvic fraction is associated with acetate accumulation and suppression of M-AsR. Although these amendments were commercially sourced and therefore cannot capture the full molecular heterogeneity and mineral association of native soil organic matter, they provide a controlled contrast between humic-like redox-active traits and fulvic-like labile traits that can also vary within native soil dissolved organic matter. This trait-based lens helps link molecular characteristics of organic inputs to environmental relevance in rice systems, where flooding, organic inputs, CH_4 cycling, and As exposure intersect. Our results support a testable premise that the molecular composition of the organic amendments, rather than amendment quantity alone, may help anticipate when organic additions are more likely to amplify CH_4-linked As release. If borne out in the field, this would motivate screening organic amendments and soil dissolved organic matter for humic-like redox-active characteristics, including quinone-like signatures and electron-accepting capacity, to flag higher-risk inputs and to inform amendment selection, blending, or processing. Establishing the generality and management utility of this framework will require field validation across soils, amendment sources, and water-management regimes.

■ ASSOCIATED CONTENT

Supporting Information

The Supporting Information is available free of charge at https://pubs.acs.org/doi/10.1021/acs.est.5c12983.

Methodological details for three experiments, including verification of the M-AsR process through stoichiometric ratio analysis, evaluation of humic acid-mediated As/Fe release in CH_4-oxidizing scorodite systems, and electrochemical measurement of the electron transfer capacity

https://doi.org/10.1021/acs.est.5c12983
Environ. Sci. Technol. 2026, 60, 10804−10815

of humic and fulvic acids (Texts S1−S3); key background information on the physicochemical properties of the soil sample and the primer-defined qPCR targets used in this study (Tables S1−S2); and additional supporting results for the spectroscopic characterization of humic and fulvic acids, acetate dynamics in anoxic soil suspensions, correlation and random forest analyses of porewater chemical indicators, dynamic variations of As species under $^{13}CH_4$ incubation, redundancy analysis of microbial community responses to environmental factors, and the electron transfer abilities of humic and fulvic acids (Figures S1−S6) (PDF)

AUTHOR INFORMATION

Corresponding Author

Xianjin Tang − *Zhejiang Provincial Key Laboratory of Agricultural Resources and Environment, Zhejiang University, Hangzhou 310058, China; Grantham Institute, Imperial College London, London SW7 2AZ, United Kingdom;* orcid.org/0000-0002-7515-2047; Email: xianjin@zju.edu.cn

Authors

Yu Zhang − *Key Laboratory of Development and Application of Rural Renewable Energy, Biogas Institute of Ministry of Agriculture and Rural Affairs, Chengdu 610041, China; Zhejiang Provincial Key Laboratory of Agricultural Resources and Environment, Zhejiang University, Hangzhou 310058, China; Grantham Institute, Imperial College London, London SW7 2AZ, United Kingdom*

Yun Chen − *Zhejiang Provincial Key Laboratory of Agricultural Resources and Environment, Zhejiang University, Hangzhou 310058, China*

Fengjie Liu − *Grantham Institute, Imperial College London, London SW7 2AZ, United Kingdom;* orcid.org/0000-0002-2359-5022

Yves Plancherel − *Grantham Institute, Imperial College London, London SW7 2AZ, United Kingdom*

Andreas Kappler − *Center for Applied Geosciences, Cluster of Excellence (EXC 3121): TERRA − Terrestrial Geo-Biosphere Interactions in a Changing World, University of Tübingen, Tübingen 72074, Germany;* orcid.org/0000-0002-3558-9500

Lina Zou − *Zhejiang Institute of Landscape Plants and Flowers, Zhejiang Academy of Agricultural Sciences, Hangzhou 311251, China*

Olubukola Oluranti Babalola − *Department of Life Sciences, Imperial College London, Berkshire SL5 7PY, U.K.; Food Security and Safety Focus Area, Faculty of Natural and Agricultural Sciences, North-West University, Mmabatho 2735, South Africa*

Ayansina Segun Ayangbenro − *Food Security and Safety Focus Area, Faculty of Natural and Agricultural Sciences, North-West University, Mmabatho 2735, South Africa;* orcid.org/0000-0002-3220-1873

Complete contact information is available at: https://pubs.acs.org/10.1021/acs.est.5c12983

Author Contributions

X.T. initiated this study; Conceptualization: Y.Z.; Methodology: Y.Z. and Y.C.; Visualization: Y.Z. and Y.C.; Data analysis and calculation: Y.Z., Y.C., and L.Z.; Writing—original draft: Y.Z.; Writing—review and editing: F.L., A.K., Y.P., O.B., A.A., and X.T.; Funding acquisition and supervision: L.Z., A.K., and X.T.

Notes

The authors declare no competing financial interest.

ACKNOWLEDGMENTS

The work was supported by the National Natural Science Foundation of China (Nos. 42477003 and 42207007), the Zhejiang Provincial Natural Science Foundation of China (LZ25D01002), and the Deutsche Forschungsgemeinschaft (DFG, German Research Foundation) under Germany's Excellence Strategy − EXC 3121 − 533771652.

REFERENCES

(1) Meharg, A. A.; Williams, P. N.; Adomako, E.; Lawgali, Y. Y.; Deacon, C.; Villada, A.; Cambell, R. C. J.; Sun, G.; Zhu, Y.; Feldmann, J.; Raab, A.; Zhao, F.; Islam, R.; Hossain, S.; Yanai, J. Geographical Variation in Total and Inorganic Arsenic Content of Polished (White) Rice. *Environ. Sci. Technol.* **2009**, *43*, 1612−1617.

(2) Zhang, S.; Zhang, J.; Niu, L.; Chen, Q.; Zhou, Q.; Xiao, N.; Man, J.; Ma, J.; Wei, C.; Zhang, S.; Luo, Y.; Yao, Y. Escalating arsenic contamination throughout Chinese soils. *Nat. Sustainability* **2024**, *7*, 766−775.

(3) Shi, L.-D.; Guo, T.; Lv, P.-L.; Niu, Z.-F.; Zhou, Y.-J.; Tang, X.-J.; Zheng, P.; Zhu, L.-Z.; Zhu, Y.-G.; Kappler, A.; Zhao, H.-P. Coupled anaerobic methane oxidation and reductive arsenic mobilization in wetland soils. *Nat. Geosci.* **2020**, *13*, 799−805.

(4) Glodowska, M.; Stopelli, E.; Schneider, M.; Rathi, B.; Straub, D.; Lightfoot, A.; Kipfer, R.; Berg, M.; Jetten, M.; Kleindienst, S.; Kappler, A.; et al. AdvectAs team members. Arsenic mobilization by anaerobic iron-dependent methane oxidation. *Commun. Earth Environ.* **2020**, *1*, No. 42.

(5) Gramss, G.; Ziegenhagen, D.; Sorge, S. Degradation of Soil Humic Extract by Wood- and Soil-Associated Fungi, Bacteria, and Commercial Enzymes. *Microb. Ecol.* **1999**, *37*, 140−151.

(6) Roden, E. E.; Kappler, A.; Bauer, I.; Jiang, J.; Paul, A.; Stoesser, R.; Konishi, H.; Xu, H. Extracellular electron transfer through microbial reduction of solid-phase humic substances. *Nat. Geosci.* **2010**, *3*, 417−421.

(7) Lovley, D. R.; Coates, J. D.; Blunt-Harris, E. L.; Phillips, E.; Woodward, J. C. Humic substances as electron acceptors for microbial respiration. *Nature* **1996**, *382*, 445−448.

(8) Lipczynska-Kochany, E. Humic substances, their microbial interactions and effects on biological transformations of organic pollutants in water and soil: A review. *Chemosphere* **2018**, *202*, 420−437.

(9) Klüpfel, L.; Piepenbrock, A.; Kappler, A.; Sander, M. Humic substances as fully regenerable electron acceptors in recurrently anoxic environments. *Nat. Geosci.* **2014**, *7*, 195−200.

(10) Aeschbacher, M.; Sander, M.; Schwarzenbach, R. P. Novel electrochemical approach to assess the redox properties of humic substances. *Environ. Sci. Technol.* **2010**, *44*, 87−93.

(11) Fan, L.; Dippold, M. A.; Ge, T.; Wu, J.; Thiel, V.; Kuzyakov, Y.; Dorodnikov, M. Anaerobic oxidation of methane in paddy soil: Role of electron acceptors and fertilization in mitigating CH_4 fluxes. *Soil Biol. Biochem.* **2020**, *141*, No. 107685.

(12) Liang, L.; Jin, Z.; Tao, Y.; Li, Y.; Zhao, Z.; Zhang, Y. Enhanced Extracellular Electron Transfer in Magnetite-Mediated Anaerobic Oxidation of Methane Coupled to Humic Substances Reduction: The Pivotal Role of Membrane-Bound Electron Transfer Proteins. *Environ. Sci. Technol.* **2024**, *58*, 17756−17765.

(13) Qiao, J.; Chen, M.; Zhong, S.; Tong, H.; Li, F. Soil Humic Acid Stimulates Potentially Active Dissimilatory Arsenate-Reducing Bacteria in Flooded Paddy Soil as Revealed by Metagenomic Stable Isotope Probing. *Environ. Sci. Technol.* **2024**, *58*, 2303−2312.

(14) Liang, M.; Guo, H.; Xiu, W. Effects of low molecular weight organic acids with different functional groups on arsenate adsorption on birnessite. *J. Hazard. Mater.* **2022**, *436*, No. 129108.
(15) Zhang, P.; Yao, W.; Yuan, S. Citrate-enhanced release of arsenic during pyrite oxidation at circumneutral conditions. *Water Res.* **2017**, *109*, 245−252.
(16) Scholz, V. V.; Meckenstock, R. U.; Nielsen, L. P.; Risgaard-Petersen, N. Cable bacteria reduce methane emissions from rice-vegetated soils. *Nat. Commun.* **2020**, *11*, No. 1878.
(17) Chen, K.-H.; Feng, J.; Huang, Q.; Tang, X.; Jia, H.; Liu, Y.-R. Coupling methane oxidation to pollutant transformation: a microbiome framework for climate mitigation and soil remediation. *Soil Environ. Health* **2026**, *4*, No. 100202.
(18) Yan, Z.; Du, K.; Yan, Y.; Huang, R.; Zhu, F.; Yuan, X.; Wang, S.; Ferry, J. G. Respiration-driven methanotrophic growth of diverse marine methanogens. *Proc. Natl. Acad. Sci. U.S.A.* **2023**, *120*, No. e1991788176.
(19) Yang, W.-t.; Shen, L.-d.; Bai, Y.-n. Role and regulation of anaerobic methane oxidation catalyzed by NC10 bacteria and ANME-2d archaea in various ecosystems. *Environ. Res.* **2023**, *219*, No. 115174.
(20) Zhou, Y.; Yuan, Z.; Jiang, O.; Chen, D.; Gustave, W.; Xu, J.; Tang, X. Elevated temperature promotes methane-dependent arsenate reduction in paddy soils. *Soil Biol. Biochem.* **2025**, *206*, No. 109800.
(21) Jiang, O.-Y.; Zhang, S.-Y.; Zhao, X.-D.; Liu, Z.-T.; Kappler, A.; Xu, J.-M.; Tang, X.-J. Arsenic Reduces Methane Emissions from Paddy Soils: Insights from Continental Investigation and Laboratory Incubations. *Environ. Sci. Technol.* **2024**, *58*, 17685−17694.
(22) Cai, C.; Leu, A. O.; Xie, G.; Guo, J.; Feng, Y.; Zhao, J.; Tyson, G. W.; Yuan, Z.; Hu, S. A methanotrophic archaeon couples anaerobic oxidation of methane to Fe(III) reduction. *ISME J.* **2018**, *12*, 1929−1939.
(23) Pienkowska, A.; Glodowska, M.; Mansor, M.; Buchner, D.; Straub, D.; Kleindienst, S.; Kappler, A. Isotopic Labeling Reveals Microbial Methane Oxidation Coupled to Fe(III) Mineral Reduction in Sediments from an As-Contaminated Aquifer. *Environ. Sci. Technol. Lett.* **2021**, *8*, 832−837.
(24) Yi, X.-Y.; Yang, Y.-P.; Yuan, H.-Y.; Chen, Z.; Duan, G.-L.; Zhu, Y.-G. Coupling metabolisms of arsenic and iron with humic substances through microorganisms in paddy soil. *J. Hazard. Mater.* **2019**, *373*, 591−599.
(25) Nordstrom, D. K.; Majzlan, J.; Konigsberger, E. Thermodynamic Properties for Arsenic Minerals and Aqueous Species. *Rev. Mineral Geochem.* **2014**, *79*, 217−255.
(26) Bi, R.; Lu, Q.; Yu, W.; Yuan, Y.; Zhou, S. Electron transfer capacity of soil dissolved organic matter and its potential impact on soil respiration. *J. Soils Sediments* **2013**, *13*, 1553−1560.
(27) Harvey, M. C.; Schreiber, M. E.; Rimstidt, J. D.; Griffith, M. M. Scorodite Dissolution Kinetics: Implications for Arsenic Release. *Environ. Sci. Technol.* **2006**, *40*, 6709−6714.
(28) Qiao, J.; Li, X.; Li, F.; Liu, T.; Young, L. Y.; Huang, W.; Sun, K.; Tong, H.; Hu, M. Humic Substances Facilitate Arsenic Reduction and Release in Flooded Paddy Soil. *Environ. Sci. Technol.* **2019**, *53*, 5034−5042.
(29) Lomax, C.; Liu, W. J.; Wu, L.; Xue, K.; Xiong, J.; Zhou, J.; McGrath, S. P.; Meharg, A. A.; Miller, A. J.; Zhao, F. J. Methylated arsenic species in plants originate from soil microorganisms. *New Phytol.* **2012**, *193*, 665−672.
(30) Caporaso, J. G.; Lauber, C. L.; Walters, W. A.; Berg-Lyons, D.; Lozupone, C. A.; Turnbaugh, P. J.; Fierer, N.; Knight, R. Global patterns of 16S rRNA diversity at a depth of millions of sequences per sample. *Proc. Natl. Acad. Sci. U.S.A.* **2011**, *108*, 4516−4522.
(31) Huang, L.; Levintal, E.; Erikson, C. B.; Coyotl, A.; Horwath, W. R.; Dahlke, H. E.; Rodrigues, J. L. M. Molecular and Dual-Isotopic Profiling of the Microbial Controls on Nitrogen Leaching in Agricultural Soils under Managed Aquifer Recharge. *Environ. Sci. Technol.* **2023**, *57*, 11084−11095.
(32) Callahan, B. J.; McMurdie, P. J.; Rosen, M. J.; Han, A. W.; Johnson, A. J. A.; Holmes, S. P. DADA2: High-resolution sample inference from Illumina amplicon data. *Nat. Methods* **2016**, *13*, 581−583.
(33) Zhang, Y.; Tong, D.; Zou, L.; Ji, H.; Zhou, X.; Gustave, W.; Tang, X. Low-molecular-weight organic acids inhibit the methane-dependent arsenate reduction process in paddy soils. *Ecotoxicol. Environ. Saf.* **2024**, *282*, No. 116716.
(34) Tong, D.; Wang, Y.; Yu, H.; Shen, H.; Dahlgren, R. A.; Xu, J. Viral lysing can alleviate microbial nutrient limitations and accumulate recalcitrant dissolved organic matter components in soil. *ISME J.* **2023**, *17*, 1247−1256.
(35) Jiang, J.; Kappler, A. Kinetics of Microbial and Chemical Reduction of Humic Substances: Implications for Electron Shuttling. *Environ. Sci. Technol.* **2008**, *42*, 3563−3569.
(36) Stern, N.; Mejia, J.; He, S.; Yang, Y.; Ginder-Vogel, M.; Roden, E. E. Dual Role of Humic Substances As Electron Donor and Shuttle for Dissimilatory Iron Reduction. *Environ. Sci. Technol.* **2018**, *52*, 5691−5699.
(37) Lu, Y.; Hu, S.; Liu, F.; Liang, Y.; Shi, Z. Effects of humic acid and fulvic acid on the sequestration of copper and carbon during the iron oxide transformation. *Chem. Eng. J.* **2020**, *383*, No. 123194.
(38) Wang, M.; Zhao, Z.; Li, Y.; Liang, S.; Meng, Y.; Ren, T.; Zhang, X.; Zhang, Y. Control the greenhouse gas emission via mediating the dissimilatory iron reduction: Fulvic acid inhibit secondary mineralization of ferrihydrite. *Water Res.* **2022**, *218*, No. 118501.
(39) Yang, J.; Zou, L.; Zheng, L.; Yuan, Z.; Huang, K.; Gustave, W.; Shi, L.; Tang, X.; Liu, X.; Xu, J. Iron-based passivator mitigates the coupling process of anaerobic methane oxidation and arsenate reduction in paddy soils. *Environ. Pollut.* **2022**, *313*, No. 120182.
(40) He, Q.; Yu, L.; Li, J.; He, D.; Cai, X.; Zhou, S. Electron shuttles enhance anaerobic oxidation of methane coupled to iron(III) reduction. *Sci. Total Environ.* **2019**, *688*, 664−672.
(41) Xie, M.; Zhang, X.; Li, S.; Maulani, N.; Cai, F.; Zheng, Y.; Cai, C.; Virdis, B.; Yuan, Z.; Hu, S. Humic substances as electron acceptor for anaerobic oxidation of methane (AOM) and electron shuttle in Mn (IV)-dependent AOM. *Sci. Total Environ.* **2024**, *912*, No. 169576.
(42) Miletić, S. B.; Spasić, S. D.; Avdalović, J.; Beškoski, V.; Ilić, M.; Gojgić-Cvijović, G.; Vrvić, M. M. Short communication the effect of humic acids on zymogenous microbial consortia growth. *CLEAN − Soil, Air, Water* **2014**, *42*, 1280−1283.
(43) Amstaetter, K.; Borch, T.; Kappler, A. Influence of humic acid imposed changes of ferrihydrite aggregation on microbial Fe(III) reduction. *Geochim. Cosmochim. Acta* **2012**, *85*, 326−341.
(44) Bauer, M.; Blodau, C. Mobilization of arsenic by dissolved organic matter from iron oxides, soils and sediments. *Sci. Total Environ.* **2006**, *354*, 179−190.
(45) Bai, Y.-N.; Wang, X.-N.; Wu, J.; Lu, Y.-Z.; Fu, L.; Zhang, F.; Lau, T.-C.; Zeng, R. J. Humic substances as electron acceptors for anaerobic oxidation of methane driven by ANME-2d. *Water Res.* **2019**, *164*, No. 114935.
(46) Pedersen, H. D.; Postma, D.; Jakobsen, R. Release of arsenic associated with the reduction and transformation of iron oxides. *Geochim. Cosmochim. Acta* **2006**, *70*, 4116−4129.
(47) Dove, P. M.; Rimstidt, J. D. The solubility and stability of scorodite, $FeAsO_4 \cdot 2H_2O$. *Am. Mineral.* **1985**, *70*, 838−844.
(48) Li, R.; Yuan, Y.; Xi, B.; Tan, W. Anaerobic methane oxidation coupled with denitrification mitigates soil nitrous oxide emissions. *Sci. Adv.* **2025**, *11*, No. eadv1410.
(49) Yu, X.; Li, J.; Zhou, Y.; Chen, Y.; Zou, L.; Luo, C.; Shen, C.; Liu, F.; Xu, J.; Tang, X. Identification of the microorganisms for methane-dependent arsenate reduction in wetland using DNA-stable isotope probing and metagenomics. *Water Res.* **2025**, *284*, No. 123934.
(50) Schorn, S.; Graf, J. S.; Littmann, S.; Hach, P. F.; Lavik, G.; Speth, D. R.; Schubert, C. J.; Kuypers, M. M. M.; Milucka, J. Persistent activity of aerobic methane-oxidizing bacteria in anoxic lake waters due to metabolic versatility. *Nat. Commun.* **2024**, *15*, No. 5293.
(51) Zhang, X.; Yuan, Z.; Hu, S. Current trends in electromicrobiology of methane oxidation. *Trends Microbiol.* **2025**, *33*, 782−795.

(52) Reis, P. C. J.; Tsuji, J. M.; Weiblen, C.; Schiff, S. L.; Scott, M.; Stein, L. Y.; Neufeld, J. D. Enigmatic persistence of aerobic methanotrophs in oxygen-limiting freshwater habitats. *ISME J.* **2024**, *18*, No. wrae041.
(53) Ettwig, K. F.; Butler, M. K.; Le Paslier, D.; Pelletier, E.; Mangenot, S.; Kuypers, M. M. M.; Schreiber, F.; Dutilh, B. E.; Zedelius, J.; de Beer, D.; Gloerich, J.; Wessels, H. J. C. T.; van Alen, T.; Luesken, F.; Wu, M. L.; van de Pas-Schoonen, K. T.; den Camp, H. J. M. O.; Janssen-Megens, E. M.; Francoijs, K.; Stunnenberg, H.; Weissenbach, J.; Jetten, M. S. M.; Strous, M. Nitrite-driven anaerobic methane oxidation by oxygenic bacteria. *Nature* **2010**, *464*, 543−548.
(54) Vaksmaa, A.; Guerrero-Cruz, S.; van Alen, T. A.; Cremers, G.; Ettwig, K. F.; Lüke, C.; Jetten, M. S. M. Enrichment of anaerobic nitrate-dependent methanotrophic 'Candidatus Methanoperedens nitroreducens' archaea from an Italian paddy field soil. *Appl. Microbiol. Biotechnol.* **2017**, *101*, 7075−7084.
(55) Ramos, H. C.; Hoffmann, T.; Marino, M.; Nedjari, H.; Presecan-Siedel, E.; Dreesen, O.; Glaser, P.; Jahn, D. Fermentative metabolism of Bacillus subtilis: physiology and regulation of gene expression. *J. Bacteriol.* **2000**, *182*, 3072−3080.
(56) Saltikov, C. W.; Newman, D. K. Genetic identification of a respiratory arsenate reductase. *Proc. Natl. Acad. Sci. U.S.A.* **2003**, *100*, 10983−10988.
(57) Rosen, B. P. Biochemistry of arsenic detoxification. *FEBS Lett.* **2002**, *529*, 86−92.
(58) Coppi, M. V.; Leang, C.; Sandler, S. J.; Lovley, D. R. Development of a Genetic System for Geobacter sulfurreducens. *Appl. Environ. Microbiol.* **2001**, *67*, 3180−3187.
(59) Krafft, T.; Macy, J. M. Purification and characterization of the respiratory arsenate reductase of Chrysiogenes arsenatis. *Eur. J. Biochem.* **1998**, *255*, 647−653.
(60) Bodelier, P. L. E.; Laanbroek, H. J. Nitrogen as a regulatory factor of methane oxidation in soils and sediments. *FEMS Microbiol. Ecol.* **2004**, *47*, 265−277.
(61) Rahman, M. T.; Crombie, A.; Moussard, H.; Chen, Y.; Murrell, J. C. Acetate Repression of Methane Oxidation by Supplemental Methylocella silvestris in a Peat Soil Microcosm. *Appl. Environ. Microbiol.* **2011**, *77*, 4234−4236.
(62) Roy, R.; Conrad, R. Effect of methanogenic precursors (acetate, hydrogen, propionate) on the suppression of methane production by nitrate in anoxic rice field soil. *FEMS Microbiol. Ecol.* **1999**, *28*, 49−61.
(63) Weng, L.; Van Riemsdijk, W. H.; Hiemstra, T. Effects of Fulvic and Humic Acids on Arsenate Adsorption to Goethite: Experiments and Modeling. *Environ. Sci. Technol.* **2009**, *43*, 7198−7204.
(64) Jin, Q.; Bethke, C. M. The thermodynamics and kinetics of microbial metabolism. *Am. J. Sci.* **2007**, *307*, 643−677.

https://doi.org/10.1021/acs.est.5c12983
Environ. Sci. Technol. 2026, 60, 10804−10815